In situ electrochemical monitoring of ROS influence in the dynamics of ascorbic acid and polyphenolic compounds in apple fruits

Antonio Doménech-Carbó*[a], Daiane Dias[b]

[a] Departament de Química analítca, Universitat de València, Dr. Moliner, 50, 46100 Burjassot (València) Spain.

[b] Laboratório de Eletro-Espectro Analítica (LEEA), Escola de Química e Alimentos, Universidade Federal do Rio Grande, Av. Itália, km 8, Rio Grande, 96203-900, RS, Brazil.

e-mail: antonio.domenech@uv.es.

Abstract

In situ recording of the voltammetric profile of different apple (*Malus domestica* Borkh.) varieties (Golden, Granny Smith, Reineta, Red delicious, Fuji, and Braeburn) without and with ROS generation is reported. The voltammetric response associated to the oxidation of ascorbic acid (AA) and polyphenolic (PPs) components was recorded. The obtained voltammetric profiles were satisfactorily fitted to a theoretical kinetic model consisting of the competing, dual activation pathways of AA and PPs followed by a degradative step. The rate constants for these processes were calculated from voltammetric data revealing significant differences between varieties. The activation pathways as well as the influence of electrochemical ROS generation on it were variety-sensitive while the degradative step was almost variety insensitive and lightly sensitive to ROS generation.

Keywords: Electrochemistry; apple; ROS; In situ; Kinetics.

1. Introduction

A plethora of compounds with antioxidant properties have been identified in apple (*Malus domestica* Borkh.) cultivars. Among them, polyphenols (mainly flavonoids and phenolic acids) Wojdy1o, Oszmianski, & Laskowski, (2008) and ascorbic acid (Fang et al. 2017). These components have important nutritional benefits and have significant potential to prevent the development of many diseases including cardiovascular and pulmonary diseases, cancer, diabetes, etc. (Boyer & Liu, 2004; Gerhauser, 2008).

A significant part of recent research is focused on the factors influencing the composition of fruits (Fand et al., 2017; Chai et al., 2020), the distribution of components (Tang& Lee, 2016), and their response to storage (Lu et al., 2021) and postharvesting treatments (Santarelli et al., 2020). Another focus of attention is the influence of such compounds in plant physiology (Mauro et al., 2016), in particular, the scavenging of reactive oxygen species (ROS) (Bi et al., 2014; Li et al., 2020).

Accordingly, there is a growing interest in the elucidation, at the genetic (Davey, 2006), epigenetic (Conklin et al., 1997), and microbioma (Yashiro, Spear, & McManus, 2011) levels, of the biosynthetic and regulatory pathways driving the presence of ascorbic acid (AA) and polyphenolic (PPs) antioxidants in fruits as well as the dynamics of their interaction with ROS. These studies are made difficult by the large inter- and intraspecific variation of the content of AA and PPs in fruit crops (Fenech et al., 2019), their location within the fruit, and the dependence of the fruit composition on the maturity stage, time since harvesting, etc. (McGhie, Hunt, & Barnett, 2005). Given the influence of these processes in the maturation and aging of fruits during transportation and storage, the detailed knowledge of these processes is of interest for food industry.

In this context, *in vivo* electrochemical methods have been extensively used to study plant physiology with particular attention to membrane potentials and transmembrane ion fluxes, evaluation of antioxidant capacities (Barros et al., 2008; Korotkova, Voronova, & Dorozhko, 2012) and monitoring H_2O_2 release (Ren et al., 2015). Complementing these approaches, we developed solid state methodologies based on the voltammetry of immobilized particles aimed to establish phylogenetic relationships (Doménech-Carbó et al., 2015a, 2017; Mateo et al., 2018), reactivity of plant extracts

with ROS (Doménech-Carbó, Gavara, Hernández, & Domínguez, 2015; Doménech-Carbó et al., 2019), and chemoecological interactions (Doménech-Carbó et al., 2015b). Inspired by this methodology, we applied in previous works an *in situ* voltammetric analysis to characterize tomato varieties (Doménech-Carbó, Domínguez, Hernández, & & Gavara, 2015) and to monitor signaling transduction of plant defense against stress in leaves of *Aloe vera* (Doménech-Carbó, Dias, & Donnici, 2021).

These last approaches are based on the record of the voltammetric response at graphite microelectrodes of electroactive organic components inserted into the subsurface region of fruits and leaves, optionally accompanied by the electrochemical generation of ROS. These can be generated by applying sufficiently cathode potential inputs to oxygen-containing solutions (Enache, Chiorcea-Paquim, Fatibello-Filho, & Oliveira-Brett, 2009; Kapałka, Foti, Comninellis, & Marselli, 2009; Marselli et al., 2003). The electrogenerated ROS can be monitored electrochemically (de Carvalho et al., 2010; Scholz et al., 2007) and the kinetics of their reaction with plant components can be modeled (Doménech-Carbó, Dias, & Donnici, 2021).

Here, we report an *in situ* electrochemical study of six apple varieties (Golden, Granny Smith, *Reineta*, Red delicious, Fugi, and Braeburn) aimed to monitor the dynamic response of antioxidant species, mainly ascorbic acid, in contact with fresh fruit sections in the absence and in the presence of electrochemically generated ROS. Significant differences were obtained between the studied apple cultivars, thus suggesting the existence of a rich dynamics in apple fruits. The voltammetric data are fitted to kinetic models providing quantitative evaluation of the reactivity of antioxidant species in the different tested varieties.

2. Material and methods

2.1. Cultivars

Fruits of apple cultivars *Malus pumila* var. Golden, Granny Smith, Reineta, Red delicious, Fuji, and Braeburn were used. Apples were harvested at optimal ripeness by different cultivars in the Valencian region (Spain), all corresponding to commercial exploitations. The fruits, whose maturity was decided by the technicians of the suppliers, were stored immediately after harvesting under a controlled atmosphere (20 ºC, rH, 5%)

with a portable thermostatic container and stored for three days under the same conditions. Five fruits of each variety from the growing seasons 2019 and 2020 were analyzed. For each variety, ten peak current vs. time curves were fitted to the theoretical kinetic model and the corresponding individual values of the rate constants were collected (vide infra).

2.2. Instrumentation and procedures

Voltammetric measurements were carried out using a three-electrode arrangement connected to a CH 720c potentiostatic device. The electrodes were two Pt microelectrodes of diameter 25 μm (CHI107) who acted as pseudo-reference and auxiliary electrodes and a graphite microelectrode of diameter 100 μm (Staedtler HB). The electrodes were inserted perpendicularly into the pericarp of each apple specimen just after its previous cut (transversal section). The three electrodes were inserted until a depth of 1 mm forming a triangle with separations of 2 mm between them. Voltammetric experiments were performed at room temperature (20 ± 1 ºC) at rH 60 %. Square wave voltammetry (SWV) was routinely used as a detection mode. Prior to electrochemical series of runs, the electrodes were immersed for 5 min in 1 M H_2SO_4. The potentials were calibrated vs. Ag/AgCl (3 M NaCl) using a 1.0 mM $K_3Fe(CN)_6$ plus 1.0 mM $K_4Fe(CN)_6$ solution in aqueous 0.10 M KCl upon recording cyclic voltammograms at glassy carbon working electrode successively employing Ag/AgCl and Pt microelectrode as a reference electrodes (see Figure S.1 in Supplementary information). Testing the detection of ascorbic acid was made by recording a set of voltammograms before and after injection of 100 μL of a 1.0 mM solution of ascorbic acid (Fluka) in the microelectrode interspace in the fruit surface.

3. Results and discussion

3.1. Voltammetric pattern and variety characterization

Firstly, the voltammetric profile of different apple varieties using *in situ* voltammetry of fresh sections of mature fruits was recorded. Figure 1 depicts the SWVs at graphite microelectrode inserted into Golden apple specimen when the potential scan was initiated at a) –0.80 V and b) 0.20 V vs. Ag/AgCl in the positive direction. In both cases, the voltammogram consists of a sharp anodic peak at 0.2 (I), followed by a broad peak

centered at ca. 0.5 V (II) and a large wave at ca. 1.2 V (III). Depending on the variety and starting potential, weaker additional peaks appear in the voltammograms (*vide infra*). Replicate experiments for different specimens of the same apple cultivar produced reasonable repeatability in the voltammetric profiles, with variations in peak potentials of 5-10 mV and maximum dispersion of peak currents around 10-15 %.

The signal I can be unambiguously assigned to the oxidation of ascorbic acid (AA), whose concentration in apples is around 10 mg per 100 g (Coseteng & Lee, 1987). This attribution was confirmed upon recording the voltammograms after the injection of 100 μL of a 1.0 mM solution of ascorbic acid near the electrodes (see Supplementary information, Figure S.2). The voltammetric signals II and III can be attributed to the oxidation of polyphenolic compounds (PPs) as judged by voltammetric data reported for catechin, chlorogenic acid, (±)-naringenin, quercetin, quercetin-3-rutinoside, naringenin, narignein chalcone, rutin and morin (Doménech-Carbó, Domínguez, Hernández, & Gavara, 2015; Doménech-Carbó, Gavara, Hernández, & Domínguez, 2015). Some of these and other electroactive compounds (epicatechin, chlorogenic acid, quercetin derivatives (galactoside, glucoside, xyloside, arabinoside, rhamnoside) and procyanidin B2, are abundant in apples (Coseteng & Lee, 1987). As already described for quercetin and chlorogenic acid, these compounds have at least one *o*-diphenol unit in common that in general electrochemically oxidizes almost reversibly to the corresponding *o*-quinone. This type of processes are represented by the peak II, resulting from the superposition of the voltammetric signals of different components. The signal III can be attributed to less reversible electrochemical oxidation processes involving other phenolic functionalities. These signals, however, can be superimposed to the oxidation of lignins and defense compounds such as salicylic acid and jasmonic acid (Doménech-Carbó, Dias, & Donnici, 2021).

In order to study the influence of ROS in fruit aging, electrochemical generation of these species was tested. According to literature (Enache, Chiorcea-Paquim, Fatibello-Filho, & Oliveira-Brett, 2009; Kapałka, Foti, Comninellis, & Marselli, 2009; Marselli et al., 2003), this phenomenon occurs in O_2-containing solutions at biological pHs when the potential scan is initiated at –0.6 V vs. Ag/AgCl or more cathodic potentials. Then, the reduction of dissolved O_2 generates superoxide radical anion, hydroperoxide radical, hydroperoxide anion and hydroxyl radical accompanying the formation of H_2O_2 and

H_2O. Under our experimental conditions, ROS can be generated in the vicinity of the working microelectrode (i.e., without affectation of the fruit at a macroscopic scale), reacting here with the fruit components. These reactions can consume several polyphenolic compounds and/or form new components, as in the case of quercetin (Krishnamachari, Levine, & Paré, 2002). The new compounds generated in the vicinity of the electrode give rise to new voltammetric signals (Doménech-Carbó, Gavara, Hernández, & Domínguez, 2015; Doménech-Carbó et al., 2019). Accordingly, the variation of the height of the signals I-III and the appearance of new anodic signals when the potential scan is initiated at sufficiently cathodic potentials, permits to monitor the interaction of ROS with polyphenolic fruit components.

Consistently, our voltammetric data reveal that the voltammograms initiated at potentials less negative than –0.5 V vs. Ag/AgCl in the positive direction display essentially identical profiles for signals I-III (no ROS generation conditions) while voltammograms initiated at more negative potentials (under ROS generation conditions) produced significant modifications in the voltammetric pattern.

Figure 2 shows the SWVs recorded for the six tested apple varieties under the conditions of ROS generation. In order to reduce the time duration of each voltammogram to facilitate the analysis (and representativity) of kinetic data (*vide infra*), the potential range was limited to the region covering the signals I and II. Interestingly, each cultivar displays a characteristic profile varying the relative intensity of such peaks and with the appearance of several additional peaks at ca. –0.2 V (IV) and –0.55 V (V) in only several varieties. Table S.1 (Supplementary information) summarizes the parameters characterizing the six cultivars in the current study. Here, the ratios between different pairs of peak currents I(I), I(II); … were taken. These currents were measured using the base lines depicted in Figure 2.

3.2. Alteration dynamics

With the intention of evaluating the influence of the time in the apples electrochemical profile, SWVs were recorded from 0 to 30 min after the cut of the specimen at intervals of 5 min initiating the potential scan either at 0.2 and –0.6 V. Figures S.1 and S.2 in

Supplementary information show the voltammograms successively recorded for specimens of the different studied varieties, scanning the potential in the positive direction. When the potential is started at 0.2 V, no electrochemical ROS generation occurs, while starting the potential at −0.6 V determines the generation of ROS at the electrode surface.

The variation of the intensity of the ascorbic acid oxidation signal (*I*(I)) with time in SWVs of the studied apple varieties initiated at 0.2 V in the positive direction is shown in Figure 3a. One can see that the peak current initially decreases for all varieties except for the Reineta one. In the case of Golden, Red Delicious and Granny Smith, the current reaches a minimum at times between 5 and 15 min and subsequently lightly increase tending to reach a maximum around 25-30 min. The Fuji and Braeburn varieties, however, solely show peak current values monotonically decreasing with time apparently tending to a certain limiting value. In contrast with all above, the *I*(I) values of *Reineta* increase until a maximum at ca. 15 min subsequently showing a slow decrease.

Figure 3b depicts the time variation of the peak current of the voltammetric signal II, *I*(II). Again, monotonically rising (Fuji), monotonically decreasing (Braeburn, Red Delicious, Granny Smith and Reineta) and an initial decrease followed by increase (Golden) patterns were recorded. Although this signal results from the superposition of the signals of several PPs, the appearance of response patterns comparable to those displayed by AA suggests that a generalized view can be adopted. Data in Figure 3 can be modeled in terms of a series of hypothesis:

a) On inserting the electrodes the compounds responsible for peaks I and II exist in different concentrations in the fruit (in the following, c^{o}_{A}).

b) The insertion of the electrodes determines in general an initial decrease of the intensity of such peaks (with few exceptions). Due to the antioxidant nature of such fruit components, this decrease can be attributed to the reaction with oxygen more or less rapidly permeating the region surrounding the working electrode.

c) More or less rapidly, depending on the apple variety, the concentration of the electroactive component A is recovered. This suggests that A is formed from at least one precursor compound.

d) The above generative/degradative pattern of the electroactive component A can be described in terms of two first-order consecutive reactions (P $\rightarrow$ A $\rightarrow$ B; Q $\rightarrow$ A $\rightarrow$ B) in which two precursor compounds, P, Q, are activated generating A which in turn degrades to a third (or more) component B.

d) Assuming that the pericarp behaves similarly to a homogeneous solution, and that the reactions proceed under pseudo first-order conditions, the variation of the concentrations of P, Q, A and B (c_P, c_Q, c_A, c_B, respectively) will be expressed by the equations:

$$\frac{dc_P}{dt} = -k_P c_P \qquad (1)$$

$$\frac{dc_Q}{dt} = -k_Q c_Q \qquad (2)$$

$$\frac{dc_A}{dt} = k_P c_P + k_Q c_Q - k_D c_A \qquad (3)$$

$$\frac{dc_B}{dt} = k_D c_A \qquad (4)$$

k_P, k_Q, k_D, being the rate constants of the consecutive steps. Assuming that initially the precursor components and the electroactive compound A are present in concentrations c^o_P, c^o_Q, c^o_A, the integration of the above equations yields for the concentration of the precursor components P, Q:

$$c_P = c^o_P e^{-k_P t} \qquad (5)$$

$$c_Q = c^o_Q e^{-k_Q t} \qquad (6)$$

Then,

$$\frac{dc_A}{dt} + k_D c_A = k_P c^o_P e^{-k_P t} + k_Q c^o_Q e^{-k_Q t} \qquad (7)$$

Multiplying the two terms of the above equation by e^{kDt} and integrating one obtains:

$$c_A = c_A^o + \frac{k_P c_P^o}{k_D - k_P}\left[e^{-k_P t} - e^{-k_D t}\right] + \frac{k_Q c_Q^o}{k_D - k_Q}\left[e^{-k_Q t} - e^{-k_D t}\right] \qquad (8)$$

This equation reduces to the well-known expression for the kinetics of two consecutive reactions when the initial concentration of A is zero and only one precursor (P) exists:

$$c_A = \frac{k_P c_P^o}{k_D - k_P}\left[e^{-k_P t} - e^{-k_D t}\right] \qquad (9)$$

A case of particular interest is when $k_D >> k_Q$. Then, Eq. (8) can be approximated by:

$$c_A \approx c_A^o + \frac{k_P c_P^o}{k_D - k_P}\left[e^{-k_P t} - e^{-k_D t}\right] + \frac{k_Q c_Q^o}{k_D} e^{-k_Q t} \qquad (10)$$

This equation predicts concentration/time curves such as that corresponding for Reineta in Figure 4a.

Assuming that the measured peak currents are proportional to the concentration of the species A, a satisfactory agreement of theory with experimental voltammetric data can be obtained taking reasonable values of the rate constants. Then, introducing an electrochemical constant, *g*. Then, Eqs. (8) and (10) can be rewritten as:

$$I = g c_A^o + g\frac{k_P c_P^o}{k_D - k_P}\left[e^{-k_P t} - e^{-k_D t}\right] + g\frac{k_Q c_Q^o}{k_D - k_Q}\left[e^{-k_Q t} - e^{-k_D t}\right] \qquad (11)$$

$$I \approx g c_A^o + g\frac{k_P c_P^o}{k_D - k_P}\left[e^{-k_P t} - e^{-k_D t}\right] + g\frac{k_Q c_Q^o}{k_D} e^{-k_Q t} \qquad (12)$$

where *I* denotes the peak current of the corresponding electrochemical process, assumed to be, proportional to the concentration of the electroactive species. This approximation yields satisfactory agreement with experimental data for AA oxidation for data in Figure 3. A representative example can be seen in Figure S.3a (Supplementary information) depicts the experimental data of the variation of *I*(I) with time for Granny Smith variety in the absence of electrochemically generated ROS. These data are superimposed to the theoretical curves from Eq. (12) taking a) $g(c^o_A + k_Q c^o_Q/k_D)$ = 1.67 μA, k_Q = 0.49 min^{-1}, $g k_P c^o_P/(k_D - k_P)$ = 0.62 μA, k_P = 0.002 min^{-1}, k_D = 0.05 min^{-1}. The resulting theoretical

curve is plotted as a continuous line while the components corresponding to the P plus D (consecutive reactions) and Q (exponential decay) terms in Eq. (12) appear as dotted lines. One can see that there is a satisfactory agreement between theory and experimental data in all cases using reasonable values of the rate constants.

Table 1 summarizes the values of the rate constants of the studied apple varieties calculated from the fit of experimental data to Eqs. (11) and (12). The listed values correspond to those averaged from ten independent sets of experimental data (for each variety, five specimens harvested in the 2019 season and five specimens from the 2020 season).

It should be noted that the content of AA can significantly vary not only among the fruits of different species, but also among varieties or cultivars from the same species (Cruz-Rus et al., 2011). It is believed that the AA content in fruits is correlated with the oxidative status of the fruit determined by the activity of enzymes involved in redox state and the H_2O_2 content (Li. et al., 2010). Under this perspective, it appears that the response to stress, although following a common pathway for all varieties, is determined by significant differences not only in the pool of AA, but also in the kinetic response expressed by the different rate constants.

Interestingly, the voltammetric features associated to PP compounds (signal II) exhibit a variation with time similar to those recorded for AA. Although a variety of components contribute to the voltammetric signal II, it appears that a generation/regeneration scheme similar to that described for AA applies. Figure S.3b shows the time variation of I(II) for Reineta variety. Experimental data can be satisfactorily fitted to Eq. (12) taking $g(c^o_A+k_Qc^o_Q/k_D)$ = 1.37 μA, k_Q = 0.32 min^{-1}, $gk_Pc^o_P/(k_D-k_P)$ = 0.93 μA, k_P = 0.004 min^{-1}, k_D = 0.20 min^{-1}. Since the signal II results from the superposition of those of different polyphenolic compounds, only apparent rate constants can be estimated. The corresponding values are summarized in Table S.2 (Supplementary information). Of course, the k_Q, k_P, k_D values listed for PPs must be seen as 'apparent', averaged values for a variety of these components and that the observed behavior does not exclude the existence of significant differences between different individual compounds.

3.3. Influence of electrochemically generated ROS

Figure 4a shows the variation of I(I) with time in SWVs of the studied apple varieties determined in SWVs such as in Figure 2 in conditions of ROS generation. One can see that the peak current/time profiles are qualitatively similar to those obtained in the absence of electrochemical ROS generation. This means that, in principle, the electrochemically generated ROS are added to the "natural" pool of ROS so that AA follows the aforementioned pathways of decay and regeneration/degradation.

Figure S.4a (Supplementary information) compares the experimental and theoretical values of I(I) for Granny Smith variety recorded in conditions of electrochemical ROS generation. The theoretical I(I) vs. time curve agrees with the theoretical one from Eq. (12) inserting $g(c^{o}_{A}+k_{Q}c^{o}_{Q}/k_{D})$ = 0.70 μA, k_{Q} = 0.11 min^{-1}, $gk_{P}c^{o}_{P}/(k_{D}-k_{P})$ = 0.42 μA, k_{P} = 0.002 min^{-1}, k_{D} = 0.05 min^{-1}. Table S.2 summarizes the values of the rate constants calculated for the studied varieties.

As in the case of AA, experimental data for the signal II, corresponding to the oxidation of PPs, I(II), can be satisfactorily fitted to Eq. (12). Figure S.4b of Supplementary information compares the experimental data for Reineta variety with theoretical (lines) a in the presence of electrochemically generated ROS. Again, experimental data can be satisfactorily fitted to theoretical ones taking $g(c^{o}_{A}+k_{Q}c^{o}_{Q}/k_{D})$ = 1.59 μA, k_{Q} = 0.38 min^{-1}, $gk_{P}c^{o}_{P}/(k_{D}-k_{P})$ = 2.2 μA, k_{P} = 0.010 min^{-1}, k_{D} = 0.20 min^{-1}. The dotted lines in Figure S.4 represent the variations of the P plus D and Q terms in Eq. (12).

3.4. Discussion

The dynamic pathway of ascorbic acid (peak I) can be interpreted considering the studies on its biosynthetic pathways and its reactivity with ROS. By the first token, there is evidence that the majority of AA in plants is mainly synthesized from D-glucose via a four-step, non-inversion pathway involving oxidation of the C1 of glucose followed by oxidation at C2 or C3, epimerization at C5 and lactonization between C1 and C4 (Loewus 1999; Wheeler, Jones, & Smirnoff, 1998). This pathway is important in plant metabolism, being also used in the synthesis of several structural cell wall

368 carbohydrates and protein glycosylation (Conklin, 2001). However, other biosynthetic
369 pathways have been recently proposed (Dowdle et al., 2007; Cruz-Rus et al., 2011). In
370 turn, AA is responsive to ROS through multiple mechanisms. The pool of AA becomes
371 increasingly because of a combination of increased oxidation and/or inefficient
372 regeneration. Formally, AA is oxidized to monodehydroascorbate which
373 disproportionates to AA and dehydroascorbate (DHA) (Fenech, Amaya, Valpuesta, &
374 Botella, 2019).
375
376 On comparing data in Table 1 one can see that the k_Q values for AA in absence of
377 electrochemical ROS generation significantly differ between the different varieties,
378 being particularly larger for Reineta. In the presence of electrochemically generated
379 ROS, the k_Q values decrease except for the variety Braeburn, being the decrease
380 particularly intense for Golden, Granny Smith and Red Delicious, as can be seen in
381 Figure S.5a of Supplementary information. In contrast, the k_P values, although
382 experiencing significant differences between varieties, are only slightly changed when
383 there is electrochemical ROS generation (See Supplementary information, Figure S.6a).
384 In turn, the values of k_D are quite homogeneous with small differences in the presence
385 and in the absence of electrochemical ROS generation (see Table 1).
386
387 The response of PPs respect to k_Q is equally dissimilar, being the values of this rate
388 constant particularly high for Fuji and Reineta (see Figures S.5 and S.6 in
389 Supplementary information). Here, ROS generation determines in general a light
390 increase of the rate constant. The values of k_P for polyphenolics are similar for all
391 pristine varieties, although high for Red Delicious and Reineta. Under conditions of
392 electrochemical ROS generation, however, the k_P values decrease significantly for these
393 two varieties as well as for Granny Smith and Braeburn. As in the case of AA, the
394 values of k_D for PPs are similar for all varieties with only light differences in the
395 presence and in the absence of electrochemical ROS generation (see Table S.2).
396
397 All these features can be interpreted on the basis of the precedent dynamic model based
398 on the existence of a dual activation pathway, expressed by the constants k_Q, k_P, for both
399 AA and PPs. The former significantly differs from one variety to another and is also
400 more sensitive to ROS, while the second is much less variety-sensitive.
401

Interestingly, on plotting the k_P values with electrochemical ROS generation vs. the k_P ones in the absence of the same for AA one obtains (see Figure 5a) that all varieties appear to be correlated, their data points falling in a common tendency curve. Since the k_P values in the absence and in the presence of electrochemically generated ROS are similar, these features suggest that the activation pathway expressed by k_P is no mediated or only slightly mediated by ROS signaling species or by species sensitive to ROS.

In contrast, when the same representation is made for PP components (Figure 5b) one can see that the varieties Golden and Fuji fall within the same tendency line produced by all varieties in the case of AA whereas the other varieties appear to define a clearly different tendency path. These features can be interpreted on assuming that the k_P dynamic path for AA also activates PPs in the case of Fuji and Golden varieties, whereas the remaining varieties do not correlate AA and PPs dynamics in the same way.

Conjointly considered, the analysis of electrochemical data presented here draws a complex scenario which can be summarized as:

a) The alteration of apple varieties in an aerobic environment follows two-step kinetics where AA and PPs are generated from two different precursors/pathways in response to stress further degrading.

b) The 'fast' activation pathway (k_Q) is strongly variety-sensitive for both AA and PPs. However, this pathway is deactivated in more or less extent by ROS in the case of AA whereas is slightly activated in the case of PPs.

c) The 'slow' activation pathway (k_P) also show sharp differences between apple varieties but becomes lightly sensitive to electrochemically generated ROS in the case of AA. In the case of PPs, the sensitivity of this pathway to ROS is considerably variety-dependent.

d) The degradative pathway (expressed by k_D values) is similar for all varieties in the case of AA and PP components. This pathway is almost insensitive to the electrochemical generation of ROS.

4. Conclusions

The in situ record of the voltammetric response of graphite microelectrodes inserted into fresh cuts of apple fruits consists of well-defined anodic peaks that can be assigned to the oxidation of ascorbic acid (AA) and polyphenolic (PP) components. The response to stress associated to such components of apple fruits was monitored by measuring the variation of the respective peak currents with time. Voltammetric measurements carried out in conditions of no ROS generation exhibit variety-characteristic differences with those performed with electrochemical ROS generation.

The dynamic response of both AA and PPs can be described in terms of a kinetic model consisting of two competing generative steps (‘relatively ‘fast’ and ‘slow’ activations of AA and PP production) followed by a degradative step. This model incorporates three variety-characteristic rate constants that can be determined from voltammetric data. The ‘fast’ activation pathway for AA is deactivated (at least partially) by electrochemically generated ROS but this effect is clearly lower or absent in the case of PPs. In contrast, the ‘slow’ activation pathway for AA is scarcely sensitive to electrochemically generated ROS while this sensitivity varies significantly between the studied apple varieties in the case of PPs. The degradative step is characterized by quite similar rate constants for both AA and PP components. This pathway becomes essentially insensitive to the electrochemical generation of ROS.

These results define a relatively complex scenario for the mechanical plus oxidative stress of apple fruits where the generation of antioxidant compounds proceeds via different generative pathways whose performance, as well as the participation of ROS, differs significantly from one to another variety. Conjointly considered, these results illustrate the capabilities of in situ voltammetry to extract information on the biochemical processes associated to plant stress and the characterization of varieties and can be relevant to monitor aging processes in food industry.

Acknowledgments: Project PID2020-113022GB-I00 supported by MCIN/ AEI /10.13039/501100011033 is gratefully acknowledged.

References

Barros, L., Falcao, S., Baptista, P., Freire, C., Vilas-Boas, M., Ferreira, I. C. F. R. (2008). Antioxidant activity of Agaricus sp. mushrooms by chemical, biochemical and electrochemical assays. *Food Chemistry*, 111, 61–66.

Bi, X., Zhang, J., Chen, C., Zhang, D., Li, P. Ma, F. (2014). Anthocyanin contributes more to hydrogen peroxide scavenging than other phenolics in apple peel. *Food Chemistry*, 152, 205–209.

Boyer, J., Liu, R. (2004). Apple phytochemicals and their health benefits. *Nutrition Journal*, 3, 5, 1–15.

Chai, Y., Chaiab, Y., Li, A., Wai, S. C., Song, C., Zhao, Y., Duan, Y., Zhang, B., Lin, Q. (2020). Cuticular wax composition changes of 10 apple cultivars during postharvest storage. *Food Chemistry*, 324, 126903.

Conklin, P. L. (2001). Recent advances in the role and biosynthesis of ascorbic acid in plants. *Plant, Cell and Environment*, 24, 383–394.

Conklin, P. L., Pallanca, J. E., Last, R. L., Smirnoff, N. (1997). L-ascorbic acid metabolism in the ascorbate-deficient arabidopsis mutant vtc1. *Plant Physiology*, 115, 1277–1285.

Coseteng, M. Y., Lee, C. Y. (1987). Changes in apple polyphenoloxidase and polyphenol concentrations in relation to degree of browning. *Journal of Food Science*, 52, 985–989.

Cruz-Rus, E., Amaya, I., Sánchez-Sevilla, J. F., Botella, M. A., Valpuesta, V. (2011). Regulation of L-ascorbic acid content in strawberry fruits. *Journal of Experimental Botany*, 62, 4191–4201.

Davey, M. W. (2006). Genetic control of fruit vitamin C contents. *Plant Physiology*, 142, 343–351.

de Carvalho, L. M., Hilgemann, M., Scholz, F., Kahlert, H., da Rosa, M. B., Wuster, M., Lindequist, U., do Nascimento, P. C., Bohrer, D. (2010). Electrochemical assay to quantify the hydroxyl radical scavenging activity of medicinal plant extracts. *Electroanalysis*, 22, 406–412.

Doménech-Carbó, A., Domínguez, I, Hernández, P., Gavara, R. (2015). Electrochemical tomato (*Solanum lycopersicum* L.) characterization using contact probe *in situ* voltammetry. *Food Chemistry*, 127, 318–325.

Doménech-Carbó, A., Gavara, R., Hernández, P., Domínguez, I. (2015). Contact probe voltammetry for *in situ* monitoring of the reactivity of phenolic tomato (*Solanum lycopersicum* L.) compounds with ROS. *Talanta*, 144, 1207-1215.

Doménech-Carbó, A., Ibars, A. M., Prieto-Mossi, J., Estrelles, E., Scholz, F., Cebrián-Torrejón, G., Martini, M. (2015a). Electrochemistry-based chemotaxonomy in plants using the voltammetry of microparticles methodology. *New Journal of Chemistry*, 39, 7421–7428.

Doménech-Carbó, A., Cebrián_Torrejón, G., Lopes-Souto, A., Martins de Moraes, M., Jorge-Kato, M., Fechine-Tavares, J., Barbosa-Filho, J. M. (2015b). Electrochemical ecology: VIMP monitoring of plant defense against external stressors. *RSC Advances*, 5, 61006–61011.

Doménech-Carbó, A., Ibars, A. M., Prieto-Mossi, J., Estrelles, E., Doménech-Carbó, M. T., Ortiz-Miranda, A. S., Lee, Y. (2017). Access to phylogeny from voltammetric fingerprints of seeds: the *Asparagus* case. *Electroanalysis*, 29, 643–650.

Doménech-Carbó, A., Cervelló-Bulls, P., González, J. M., Soriano, P., Estrelles, E., Montoya, N. (2019). Electrochemical monitoring of ROS influence on seedlings and germination response to salinity stress of three species of the tribe Inuleae. *RSC Advances*, 9, 17856-17867.

Doménech-Carbó, A., Dias, D., Donnici, M. (2021). In vivo electrochemical monitoring of signaling transduction of plant defense against stress in leaves of *Aloe vera* L. *Electroanalysis*, 33, 1024–1032.

Dowdle, J., Ishikawa, T., Gatzek, S., Rolinski, S., Smirnoff, N. (2007). Two genes in Arabidopsis thaliana encoding GDP-L-galactose phosphorylase are required for ascorbate biosynthesis and seedling viability. *Plant Journal*, 52, 673–689.

Enache, T. A., Chiorcea-Paquim, A. M., Fatibello-Filho, O., Oliveira-Brett, A. M. (2009). Hydroxyl radicals electrochemically generated in situ on a boron doped diamond electrode. *Electrochemistry Communications*, 11, 1342–1345.

Fang, T., Zhen, Q., Liao, L., Owiti, A., Zhao, L., Korban, S. S., Han, Y. (2017). Variation of ascorbic acid concentration in fruits of cultivated and wild apples. *Food Chemistry*, 225, 132–137.

Fenech, M., Amaya, I., Valpuesta, V., Botella, M. A. (2019). Vitamin C Content in Fruits: Biosynthesis and Regulation. *Frontiers in Plant Science*, 9, 2006.

Gerhauser, C. (2008). Cancer chemopreventive potential of apples, apple juice, and apple components. *Planta Medica*, 74, 1608–1624.

Kapałka, A., Foti, G., Comninellis, C. (2009). The importance of electrode material in environmental electrochemistry: Formation and reactivity of free hydroxyl radicals on boron-doped diamond electrodes. *Electrochimica Acta*, 54, 2018–2023.

Korotkova, E. I., Voronova, O. A., Dorozhko, E. V. (2012). Study of antioxidant properties of flavonoids by voltammetry. *Journal of Solid State Electrochemistry*, 16, 2435–2440.

570 Krishnamachari, V., Levine, L. H., Paré, P. W. (2002). Flavonoid oxidation by
571 theradical generator AIBN: a unified mechanism for quercetin radical scavenging.
572 *Journal of Agricultural and Food Chemistry*, 50, 4357–4363.
573
574 Li, M., Ma, F., Liang, D., Li, J., Wang, Y. (2010). Ascorbate biosynthesis during early
575 fruit development is the main reason for its accumulation in kiwi. *PLoS One*, 5, e14281.
576
577 Li, C., Wei, M., Ge, Y., Zhao, J., Chen, Y., Hou, J., Cheng, Y., Chen, J., Li, J. (2020).
578 The role of glucose-6-phosphate dehydrogenase in reactive oxygen species metabolism
579 in apple exocarp induced by acibenzolar-S-methyl. *Food Chemistry*, 308, 125663.
580
581 Loewus F. A. (1999). Biosynthesis and metabolism of ascorbic acid in plants and of
582 analogs of ascorbic acid in fungi. *Phytochemistry*, 52**,** 193–210.
583
584 Lu, L., Zuo, W., Wang, C., Li, C., Feng, T., Li, X., Wang, C., Yao, Y., Zhang, Z., Chen,
585 X. (2021). Analysis of the postharvest storage characteristics of the new red-fleshed
586 apple cultivar 'meihong'. *Food Chemistry*, 354, 129470.
587
588 Marselli, B., Garcia-Gomez, J., Michaud, P. A., Rodrigo, M. A., Comninellis, C. (2003).
589 Electrogeneration of hydroxyl radicals on boron-doped diamond electrodes, *Journal of*
590 *the Electrochemical Society*, 150, D79–D83.
591
592 Mateo, E. M., Gómez, J. V., Montoya, N., Mateo-Castro, R., Gimeno-Adelantado, J. V.,
593 Jiménez, M., Doménech-Carbó, A. (2018). Electrochemical identification of toxigenic
594 fungal species using solid-state voltammetry strategies. *Food Chemistry*, 267, 91–100.
595
596 Mauro, M. A., Dellarosa, N., Tylewicz, U., Tappi, S., Laghi, L., Rocculi, P., Rosa, M. D.
597 (2016). Calcium and ascorbic acid affect cellular structure and water mobility in apple
598 tissue during osmotic dehydration in sucrose solutions. *Food Chemistry*, 195, 19–28.
599
600 McGhie, T. K., Hunt, M., Barnett, L. E. (2005). Cultivar and growing region determine
601 the antioxidant polyphenolic concentration and composition of apples grown in New
602 Zealand. *Journal of Agricultural and Food Chemistry*, 53, 3065–3070.
603
604 Ren, Q. -Q., Huang, X. -R., Liu, G. -C., Jun, O. -Y., Li, M. -T., Chen, H., Zhao, Y. -D.,
605 Chen, W. (2015). A field-compatible technique using an electrochemical sensing
606 microbundle for real-time and simultaneous in vivo measurement of hydrogen peroxide,
607 nitric oxide, and pH under drought stress. *Sensors Actuators, B Chemical*, 220, 743–748.
608
609 Santarelli, V., Neri, L., Sacchetti, G., Mattia, C. D. D., Mastrocola, D., Pittia, P. (2020).
610 Response of organic and conventional apples to freezing and freezing pre-treatments:
611 Focus on polyphenols content and antioxidant activity. *Food Chemistry*, 308, 125570.
612
613 Scholz, F., González, G. L. L., de Carvalho, L. M., Hilgemann, M., Brainina, Kh. Z.,
614 Kahlert, H., Jack, R. S., Minh, D. T. (2007). An electrochemical system to detect free
615 radicals and radical scavengers in solution. *Angewandte Chemie International Edition*,
616 46, 8079–8082.
617

Tang, S., Lee, H. K. (2016). Syringe needle-based sampling coupled with liquid-phase extraction for determination of the three-dimensional Distribution of L-ascorbic acid in apples. *Food Chemistry*, 199, 533–540.

Wheeler, G. L., Jones, M. A., Smirnoff, N. (1998). The biosynthetic pathway of vitamin C in higher plants. *Nature*, 393**,** 365–369.

Wojdy1o, A., Oszmianski, J., Laskowski, P. (2008). Polyphenolic compounds and antioxidant activity of new and old apple varieties. *Journal of Agricultural and Food Chemistry*, 56, 6520–6530.

Yashiro, E., Spear, R. N., McManus, P. S. (2011). Culture-dependent and culture-independent assessment of bacteria in the apple phyllosphere. *Journal of Applied Microbiology*, 110, 1284–1296.

Table 1. Rate constants for AA evolution. a) No electrochemically generated ROS; b) with electrochemical generation of ROS. Averaged from ten independent sets of experimental data for each apple variety (five specimens harvested in the 2019 season and five specimens from the 2020 season).

a)

Variety	k_Q / **min**$^{-1}$	k_P / **min**$^{-1}$	k_D / **min**$^{-1}$
Golden	0.211±0.008	0.0020±0.0003	0.050±0.003
Fuji	0.040±0.04	0.014±0.002	0.20±0.02
Granny Smith	0.11±0.02	0.0020±0.0003	0.050±0.004
Braeburn	0.065±0.004	0.011±0.004	0.19±0.04
Red Delicious	0.194±0.014	0.0017±0.0004	0.10±0.04
Reineta	0.5±0.1	0.020±0.004	0.15±0.04

b)

Variety	k_Q / **min**$^{-1}$	k_P / **min**$^{-1}$	k_D / **min**$^{-1}$
Golden	0.028±0.003	0.0010±0.0003	0.050±0.003
Fuji	0.033±0.005	0.012±0.003	0.20±0.02
Granny Smith	0.041±0.003	0.0020±0.0004	0.050±0.004
Braeburn	0.081±0.013	0.008±0.001	0.20±0.04
Red Delicious	0.039±0.004	0.0010±0.0002	0.10±0.02
Reineta	0.4±0.1	0.020±0.002	0.10±0.02

Figures

Figure 1. SWVs at graphite microelectrode inserted into Golden apple specimen after semi-derivative convolution. Potential scan initiated at: a) –0.60 V and b) 0.20 V vs. Ag/AgCl in the positive direction; potential step increment 4 mV, square wave amplitude 25 mV; frequency 10 Hz. The dotted lines mark the respective starting potentials and the arrows the direction of the potential scan.

Figure 2. SWVs, at graphite microelectrode under ROS generation conditions, of: a) Golden, b) Granny Smith, c) *Reineta*, d) Red delicious, e) Fuji and f) Braeburn apple specimens after semi-derivative convolution. Potential scan initiated at –0.80 V in the positive direction; potential step increment 4 mV, square wave amplitude 25 mV; frequency 10 Hz.

Figure 3. Variation of a) I(I) and b) I(II) with time in SWVs of the different apple varieties initiated at 0.2 V vs. Ag/AgCl in the positive direction (conditions of no ROS generation).

Figure 4. Variation of a) I(I) and b) I(II) with time in SWVs of the different apple varieties initiated at –0.6 V vs. Ag/AgCl in the positive direction in conditions of electrochemical ROS generation.

Figure 5. Plots of k_P values determined under conditions of electrochemical ROS generation vs. the values of this quantity when no electrochemical ROS generation was applied for a) AA, b) PPs. The continuous lines in both a) and b) correspond to the fit of data points for AA to a polynomial function. The dotted line in b) represents a tentative tendency curve for apple varieties diverging from the above tendency curve.

Figure 1.

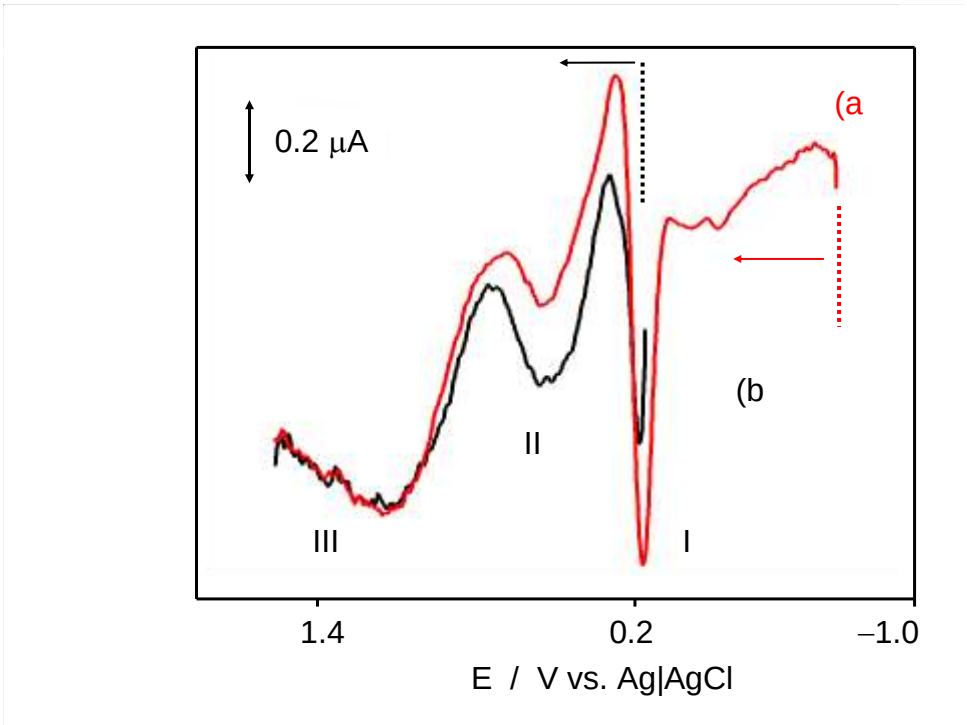

Figure 2.

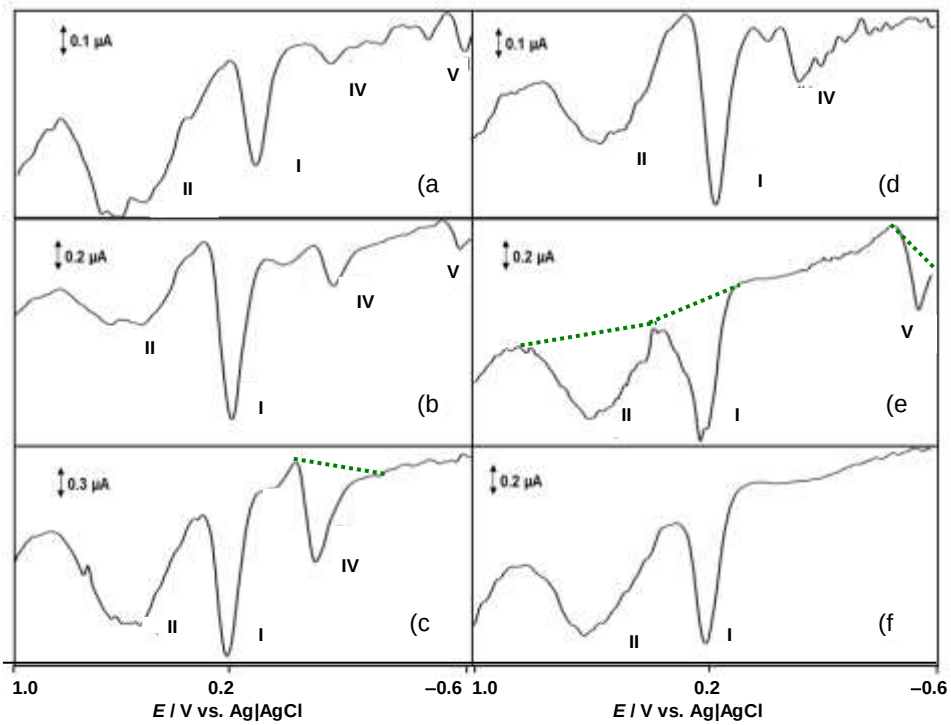
0.1 μA
V
IV
II
I
(a
0.1 μA
IV
II
I
(d
0.2 μA
V
IV
II
I
(b
0.2 μA
V
II
I
(e
0.3 μA
IV
II
I
(c
0.2 μA
II
I
(f
1.0
0.2
–0.6
E / V vs. Ag|AgCl
1.0
0.2
–0.6
E / V vs. Ag|AgCl

Figure 3.

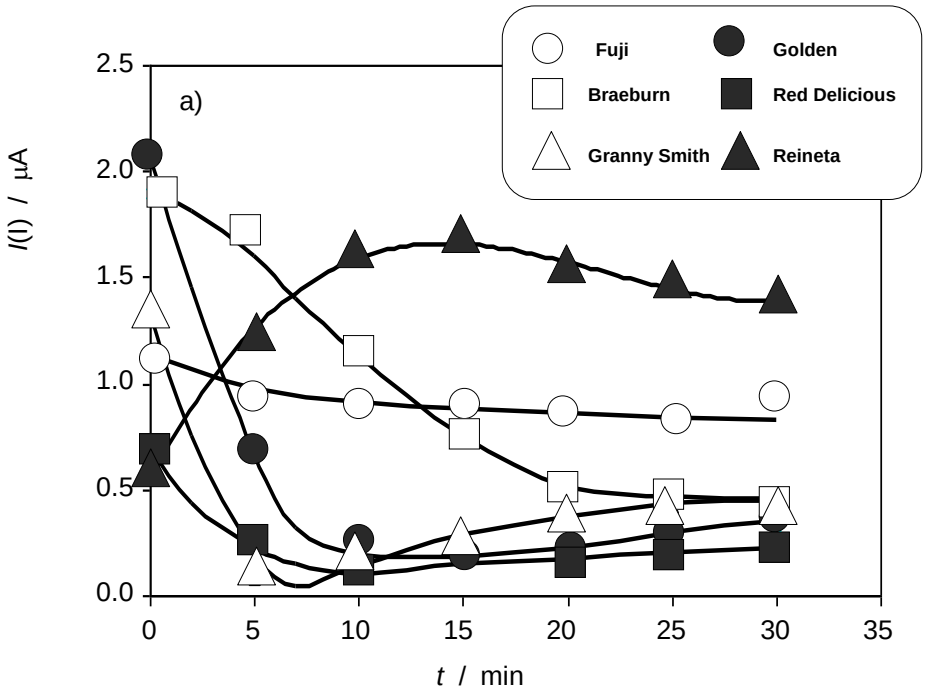
a)
Fuji
Golden
Braeburn
Red Delicious
Granny Smith
Reineta
I(I) / µA
t / min

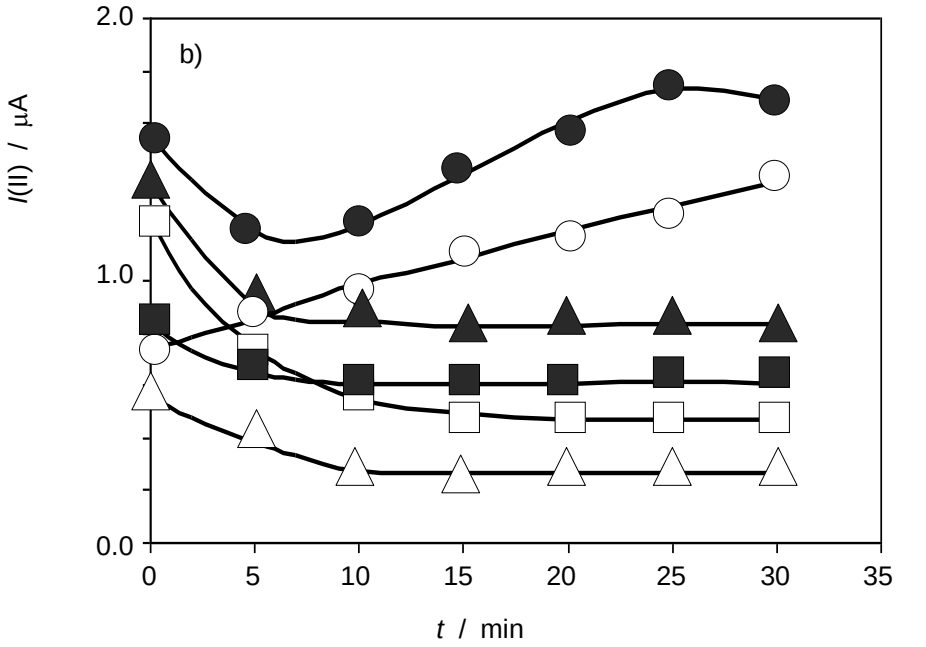
b)
I(II) / µA
t / min

Figure 4.

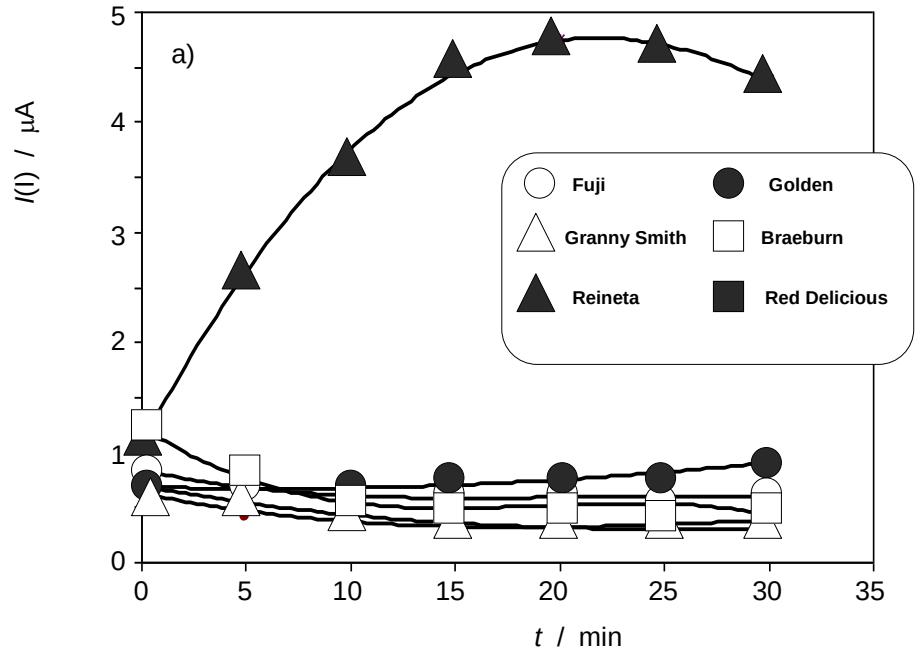
a)
I(I) / µA
t / min
Fuji
Golden
Granny Smith
Braeburn
Reineta
Red Delicious

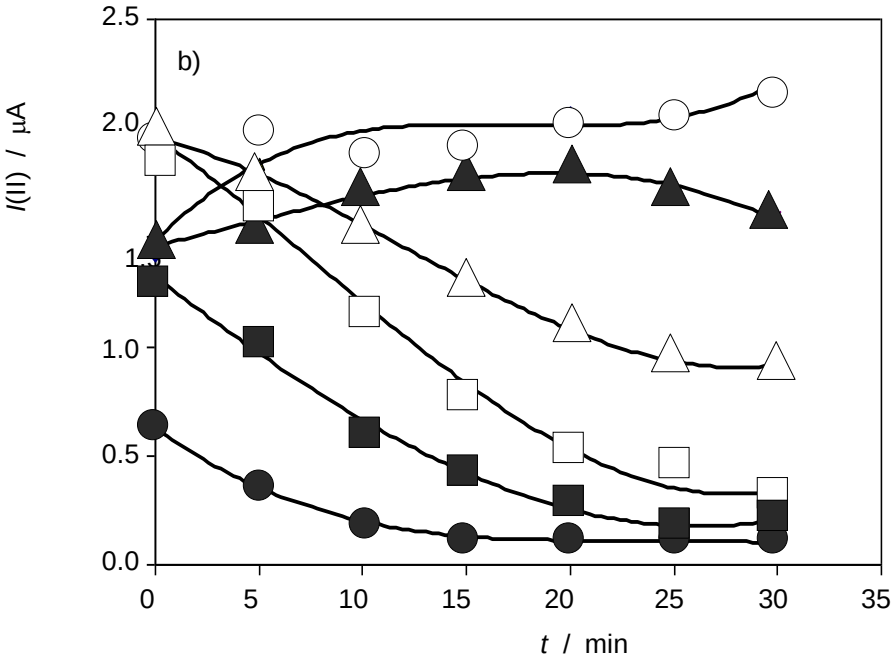
b)
I(II) / µA
t / min

Figure 5.

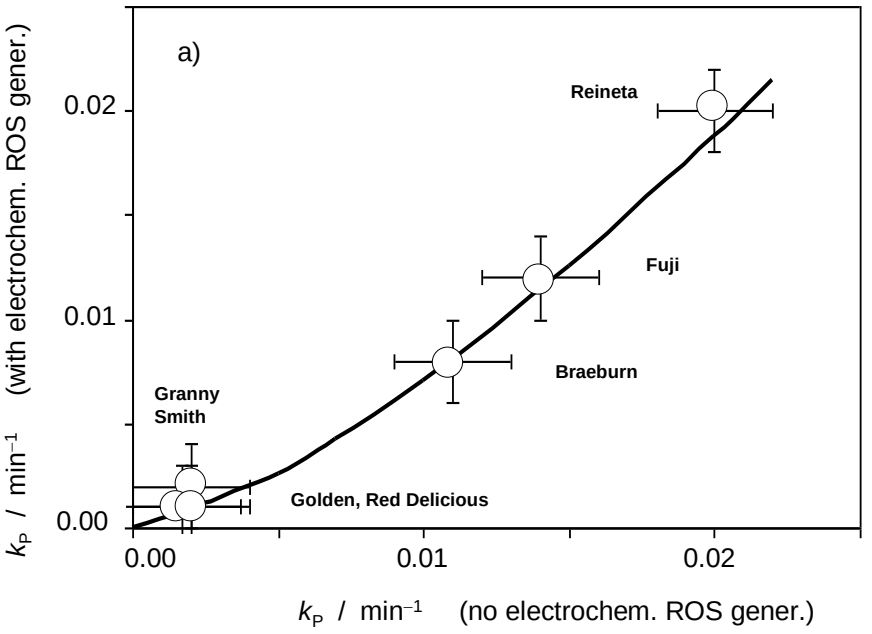
a)
Reineta
Fuji
Braeburn
Granny Smith
Golden, Red Delicious
0.02
0.01
0.00
0.00
0.01
0.02
k_P / min^{-1} (with electrochem. ROS gener.)
k_P / min^{-1} (no electrochem. ROS gener.)

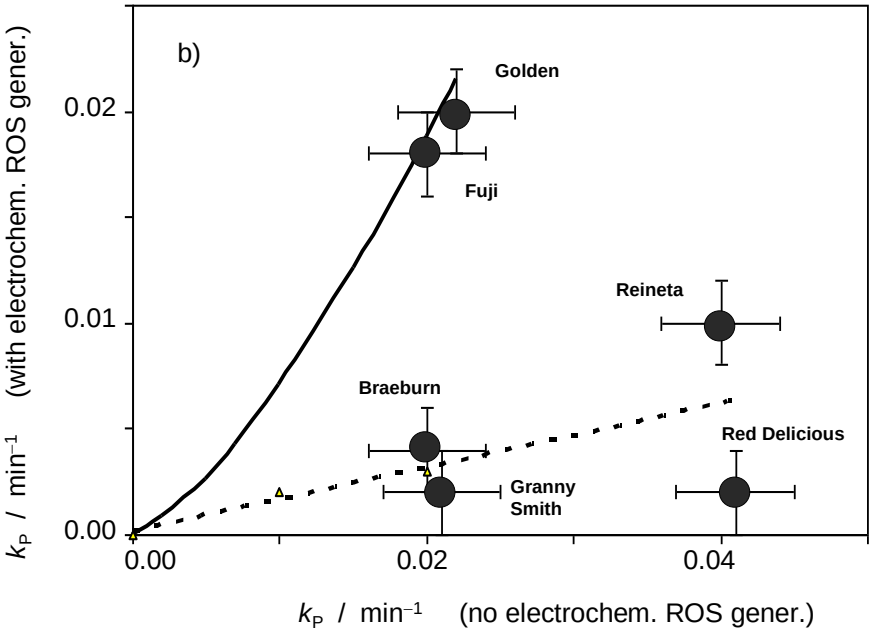
b)
Golden
Fuji
Reineta
Braeburn
Red Delicious
Granny Smith
0.02
0.01
0.00
0.00
0.02
0.04
k_P / min^{-1} (with electrochem. ROS gener.)
k_P / min^{-1} (no electrochem. ROS gener.)

Supplementary information

Figure S.1. Cyclic voltammograms at glassy carbon working electrode of 1.0 mM $K_3Fe(CN)_6$ plus 1.0 mM $K_4Fe(CN)_6$ solution in aqueous 0.10 M KCl using a) Ag/AgCl (3 M NaCl), and b) Pt microelectrode, as a reference electrode. Potential scan rate 50 mV s^{-1}.

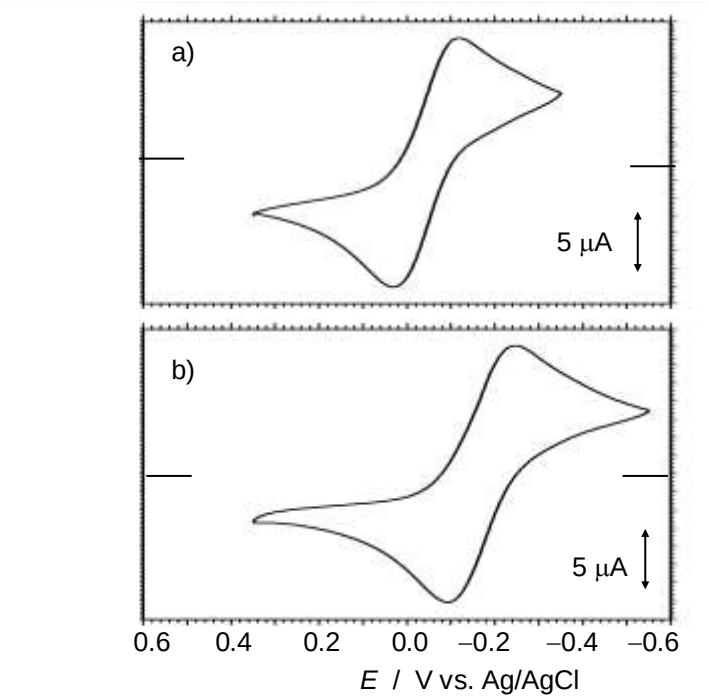

Figure S.2. SWVs at graphite microelectrode inserted into Golden apple specimen a) before, and b) after injection in the microelectrodes inter-space of 100 μL of a freshly prepared 1.0 mM solution of ascorbic acid. Potential scan initiated at –0.45 V vs. Ag/AgCl in the positive direction; potential step increment 4 mV, square wave amplitude 25 mV; frequency 10 Hz.

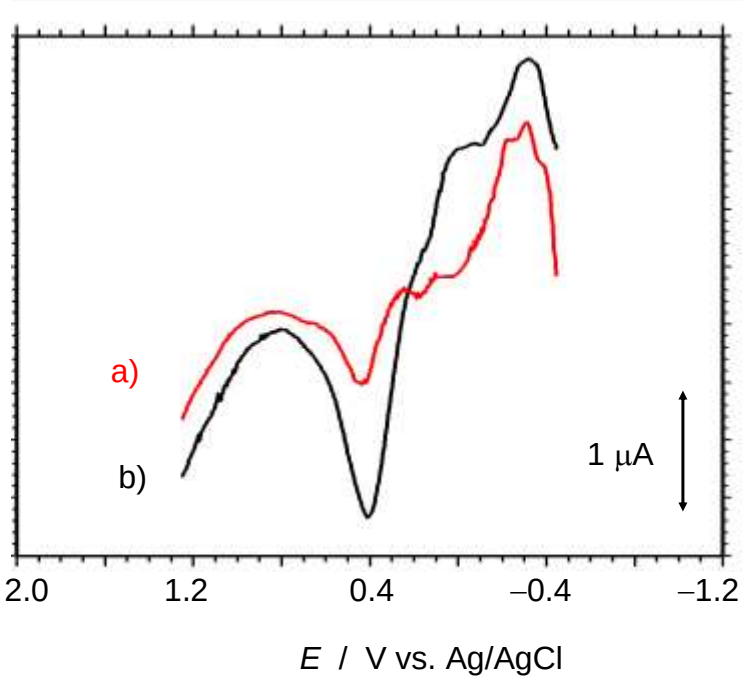

Figure S.3. Experimental (circles) and theoretical variation of a) I(I) with time for Granny Smith and b) I(II) with time for Reineta variety in both cases in the absence of electrochemically generated ROS. Continuous lines: theoretical curves from Eq. (12) taking a) $g(c^{o}_{A}+k_{Q}c^{o}_{Q}/k_{D})$ = 1.67 μA, k_{Q} = 0.49 min^{-1}, $gk_{P}c^{o}_{P}/(k_{D}-k_{P})$ = 0.62 μA, k_{P} = 0.002 min^{-1}, k_{D} = 0.05 min^{-1}, b) $g(c^{o}_{A}+k_{Q}c^{o}_{Q}/k_{D})$ = 1.37 μA, k_{Q} = 0.32 min^{-1}, $gk_{P}c^{o}_{P}/(k_{D}-k_{P})$ = 0.93 μA, k_{P} = 0.004 min^{-1}, k_{D} = 0.20 min^{-1}. The dotted lines represent the variations of the P plus D and Q terms in Eq. (12).

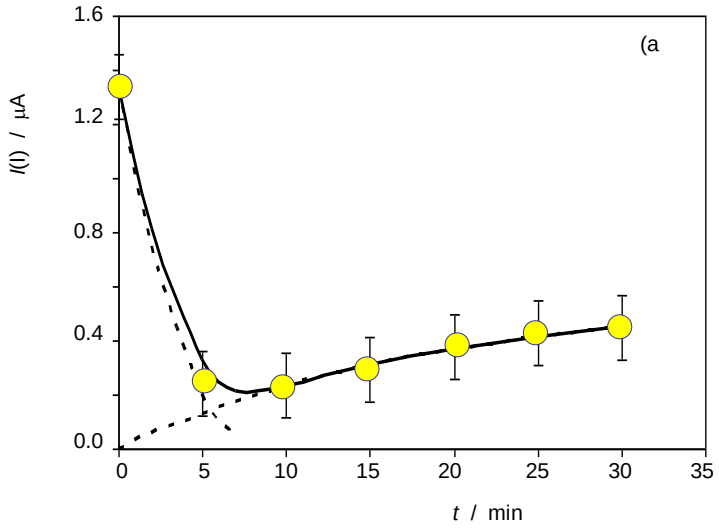

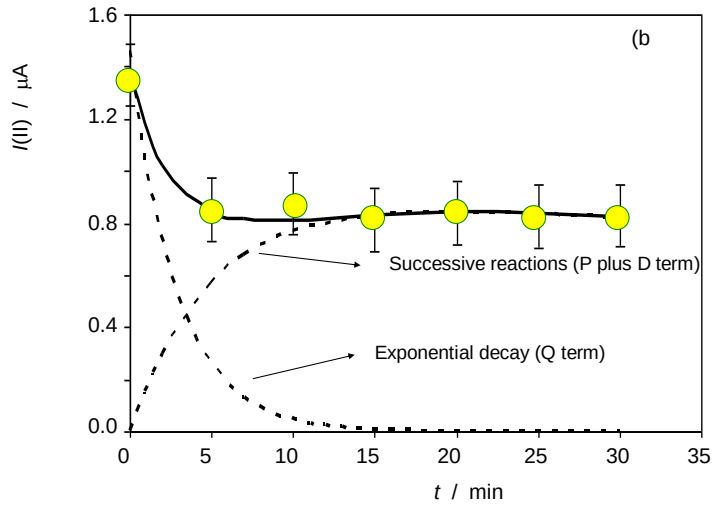

Figure S.4. Experimental (circles) and theoretical variation of a) I(I) with time for Granny Smith and b) I(II) with time for Reineta variety in both cases in the presence of electrochemically generated ROS. Continuous lines: theoretical curves from Eq. (12) taking a) $g(c^{o}_{A}+k_{Q}c^{o}_{Q}/k_{D})$ = 0.70 μA, k_{Q} = 0.11 min^{-1}, $gk_{P}c^{o}_{P}/(k_{D}-k_{P})$ = 0.42 μA, k_{P} = 0.002 min^{-1}, k_{D} = 0.05 min^{-1}, b) $g(c^{o}_{A}+k_{Q}c^{o}_{Q}/k_{D})$ = 1.59 μA, k_{Q} = 0.38 min^{-1}, $gk_{P}c^{o}_{P}/(k_{D}-k_{P})$ = 2.2 μA, k_{P} = 0.010 min^{-1}, k_{D} = 0.20 min^{-1}. The dotted lines represent the variations of the P plus D and Q terms in Eq. (12).

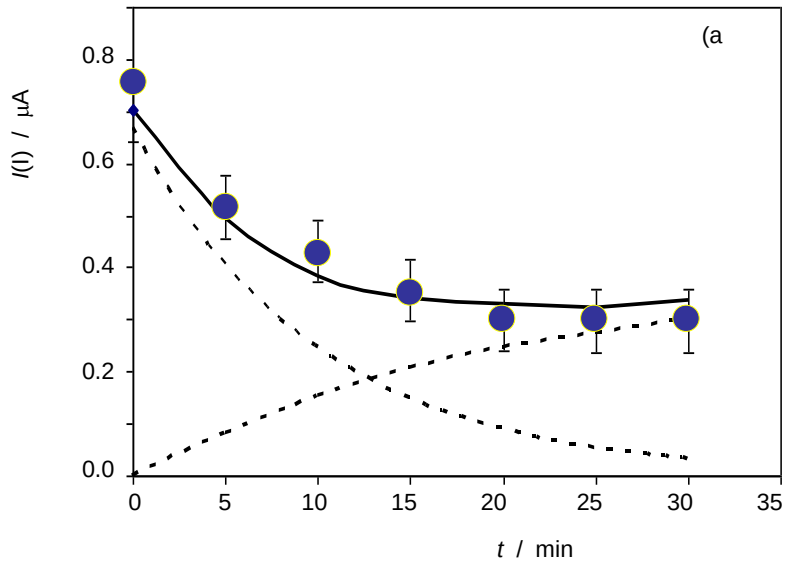

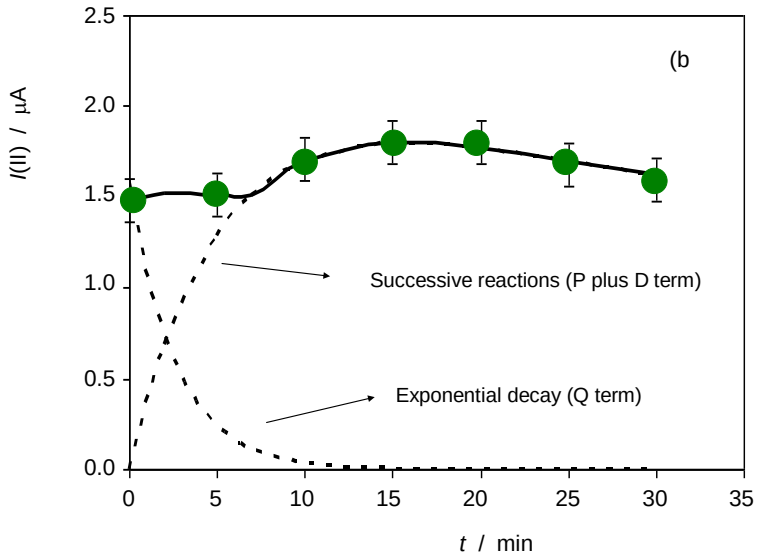

Figure S.5. k_Q values calculated for : a) AA dynamics, and b) PPs dynamics in the absence (left column) and in the presence (right column) of electrochemical ROS generation.

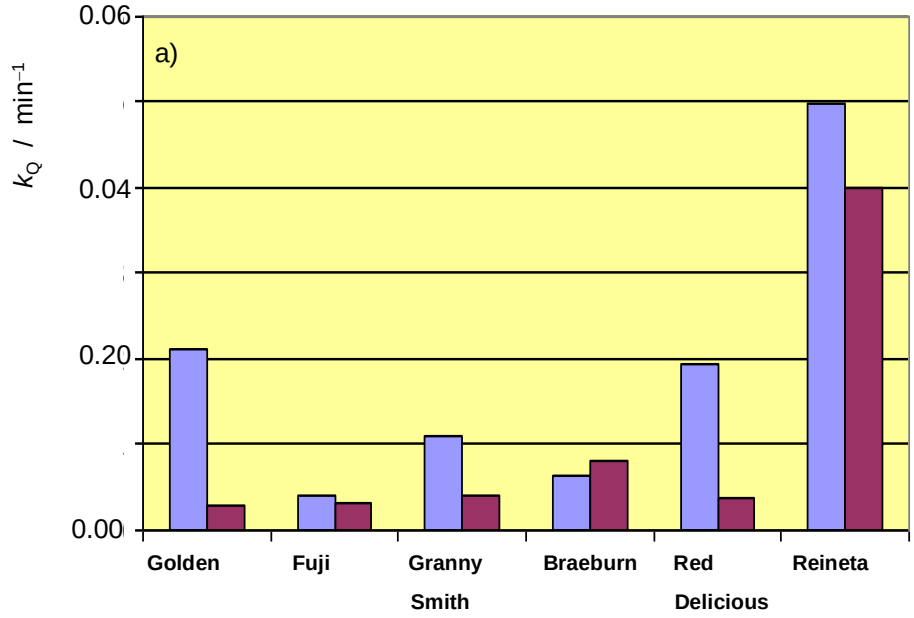

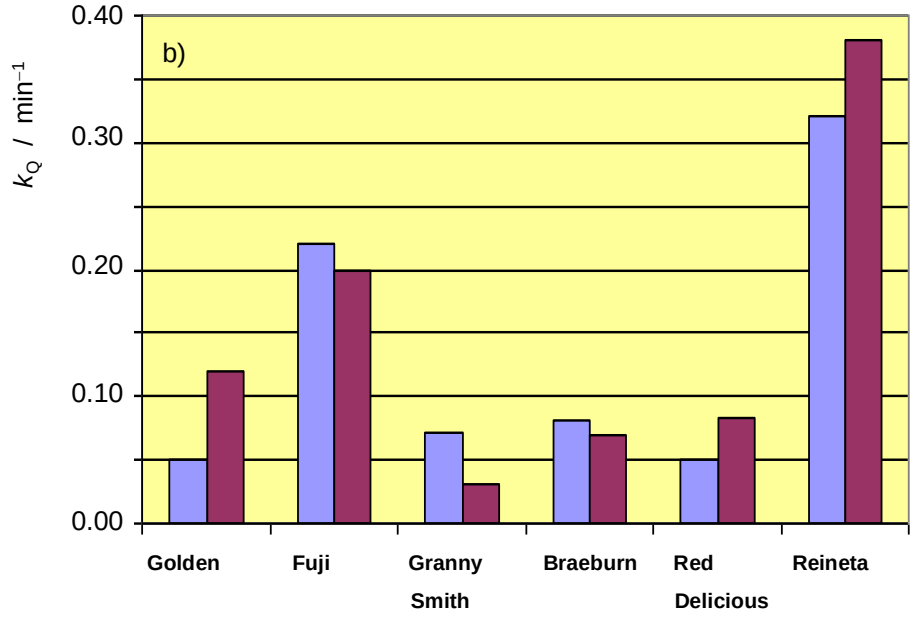

Figure S.6. k_P values calculated for : a) AA dynamics, and b) polyphenolic components dynamics in the absence (left column) and in the presence (right column) of electrochemical ROS generation.

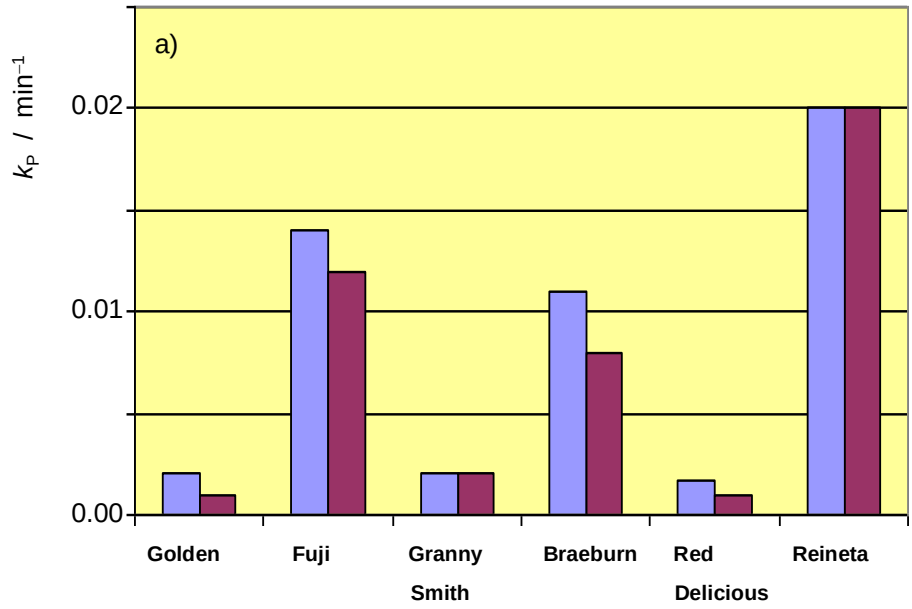

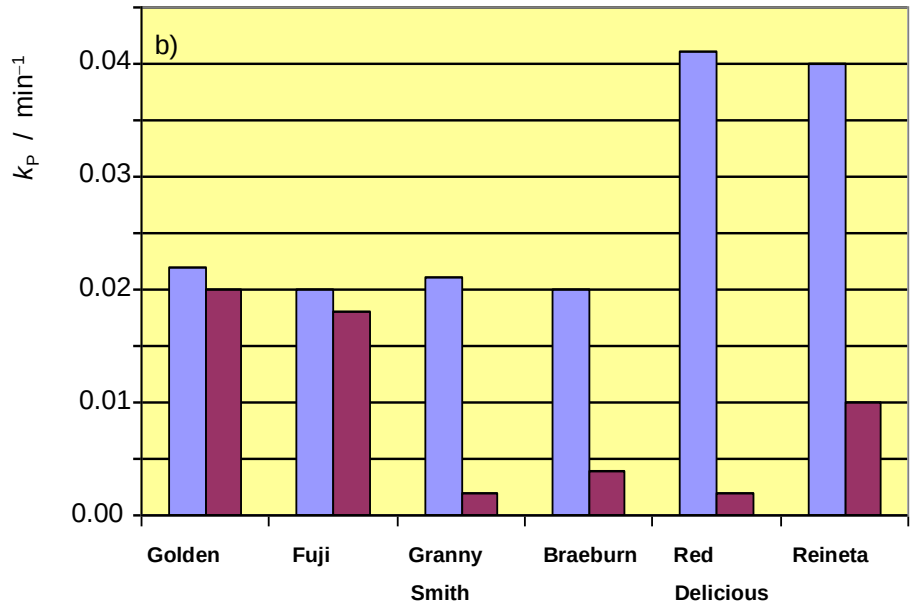

Table S.1. Voltammetric features representative of variety-characteristic voltammetric profiles. From voltammetric data in conditions such as in Figure 3. Averaged values from replicate experiments in five specimens of each apple variety.

Apple variety	***I*(II)/*I*(I)**	***I*(IV)/*I*(I)**	***I*(V)/*I*(I)**
Golden	1.1±0.2	0.24±0.04	0.38±0.06
Granny Smith	0.36±0.06	0.24±0.04	0.15±0.03
Reineta	0.68±0.08	0.58±0.07	0.00±0.02
Red Delicious	0.53±0.06	0.26±0.04	0.06±0.04
Fuji	0.65±0.08	0.00±0.02	0.40±0.06
Braeburn	0.61±0.07	0.00±0.02	0.00±0.02

Table S.2. Rate constants for PP kinetics. a) No electrochemically generated ROS; b) with electrochemical generation of ROS.

a)

Variety	k_Q / **min**$^{-1}$	k_P / **min**$^{-1}$	k_D / **min**$^{-1}$
Golden	0.051±0.006	0.022±0.003	0.071±0.004
Fuji	0.22±0.06	0.020±0.002	0.050±0.003
Granny Smith	0.072±0.006	0.021±0.002	0.20±0.03
Braeburn	0.081±0.004	0.020±0.002	0.20±0.03
Red Delicious	0.050±0.005	0.041±0.002	0.20±0.04
Reineta	0.32±0.04	0.040±0.002	0.20±0.04

b)

Variety	k_Q / **min**$^{-1}$	k_P / **min**$^{-1}$	k_D / **min**$^{-1}$
Golden	0.12±0.02	0.020±0.002	0.20±0.02
Fuji	0.20±0.06	0.018±0.003	0.070±0.004
Granny Smith	0.030±0.004	0.0020±0.0002	0.21±0.03
Braeburn	0.070±0.006	0.0040±0.0004	0.25±0.04
Red Delicious	0.083±0.004	0.0020±0.0002	0.20±0.02
Reineta	0.38±0.04	0.010±0.002	0.20±0.02